Electron Shuttle in N-Heteroaromatic Ni Catalysts for Alkene Isomerization

Maxime Tricoire, Ding Wang, Thayalan Rajeshkumar, Laurent Maron, Grégory Danoun, Grégory Nocton

JACS Au
AN OPEN ACCESS JOURNAL OF THE AMERICAN CHEMICAL SOCIETY

pubs.acs.org/jacsau

Article

Electron Shuttle in *N*-Heteroaromatic Ni Catalysts for Alkene Isomerization

Maxime Tricoire, Ding Wang, Thayalan Rajeshkumar, Laurent Maron,* Grégory Danoun,* and Grégory Nocton*

Cite This: *JACS Au* 2022, 2, 1881−1888

Read Online

ACCESS | Metrics & More | Article Recommendations | Supporting Information

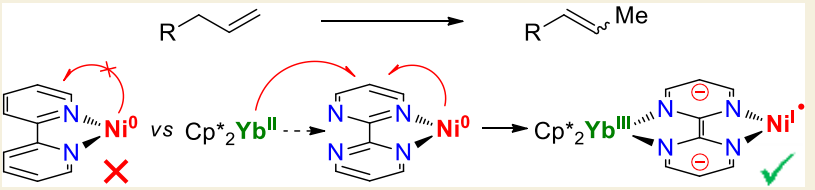

ABSTRACT: Simple *N*-heteroaromatic Ni(II) precatalysts, (L)$NiMe_2$ (L = bipy, bipym), were used for alkene isomerization. With an original reduction method using a simple borane (HB(Cat)), a low-valent Ni center was formed readily and showed good conversion when a reducing divalent lanthanide fragment, Cp^*_2Yb, was coordinated to the (bipym)$NiMe_2$ complex, a performance not achieved by the monometallic (bipy)$NiMe_2$ analogue. Experimental mechanistic investigations and computational studies revealed that the redox non-innocence of the L ligand triggered an electron shuttle process, allowing the elusive formation of Ni(I) species that were central to the isomerization process. Additionally, the reaction occurred with a preference for mono-isomerization rather than chain-walking isomerization. The presence of the low-valent ytterbium fragment, which contributed to the formation of the electron shuttle, strongly stabilized the catalysts, allowing catalytic loading as low as 0.5%. A series of alkenes with various architectures have been tested. The possibility to easily tune the various components of the heterobimetallic catalyst reported here, the ligand L and the divalent lanthanide fragment, opens perspectives for further applications in catalysis induced by Ni(I) species.

KEYWORDS: *nickel, heterometallic complexes, catalysis, alkene isomerization, redox-active ligand*

1. INTRODUCTION

To limit the use of rare metals, the chemistry of transition-metal catalysts focused on the earth-abundant metals of the first row.[1] Not only that they advantageously replace their heavier analogues, but they also constitute a formidable opportunity to develop new transformations. Among them, nickel chemistry is particularly appealing because of the possibility for the metal to enable multiple oxidation states with possible single-electron transfer (SET) reactions. For instance, nickel complexes at the formal +III and +IV oxidation states[2−5] are highly sought as they are proposed intermediates in many original cross-coupling reactions.[6−8]

In such transformations, the choice of the ligand is crucial because the metal−ligand pair often contributes to the stabilization of the unusual redox state and its subsequent reactivity. Meanwhile, the concept of redox non-innocence[9,10] showed that electronic intramolecular transfers would allow two-electron transformations with non-noble metals such as iron,[11] single-electron transformation with noble metals,[12,13] or umpolung substrate reactivity.[14,15] In nickel chemistry, the group of Vicic showed that the use of *N*-heteroaromatics allowed manipulating the metallic redox state because of ligand redox effects.[16,17] Depending on the coordination environment, the electron is either metal- or ligand-centered, allowing adapting oxidation states from +I to +III for each elementary mechanistic step (Scheme 1, top).[18] Controlling these electronic shuttles is key for tuning reactivity.

Likewise, some of us recently developed a series of compounds, in which the reactive transition-metal ion is coordinated to a redox-active *N*-heteroaromatic ligand, the electronics of which are modulated by the presence of a low-valent lanthanide. This strategy has been used to stabilize Pd^{IV} species[19] as well as enhance the reductive elimination of Ni^{II} alkyl species after CO insertion, the kinetics of which are hampered by the presence of the lanthanide fragment.[20] In this example, the *N*-heterocyclic ligand is the 2,2′-bipyrimidine (bipym), forming the Ln(bipym)$NiMe_2$ complex in which the lanthanide fragment (Ln) is the Cp^*_2Yb, an f^{14} diamagnetic complex.[21] The electron transfer occurs readily upon coordination of the divalent lanthanide ion so that the bipym ligand is reduced by one electron, while the ytterbium becomes f^{13} and

Received: April 27, 2022
Revised: May 25, 2022
Accepted: May 27, 2022
Published: August 10, 2022

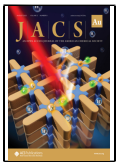

https://doi.org/10.1021/jacsau.2c00251
JACS Au 2022, 2, 1881−1888

Scheme 1. Possible Electron Shuttles between a Ni Center and Redox-Active Ligands

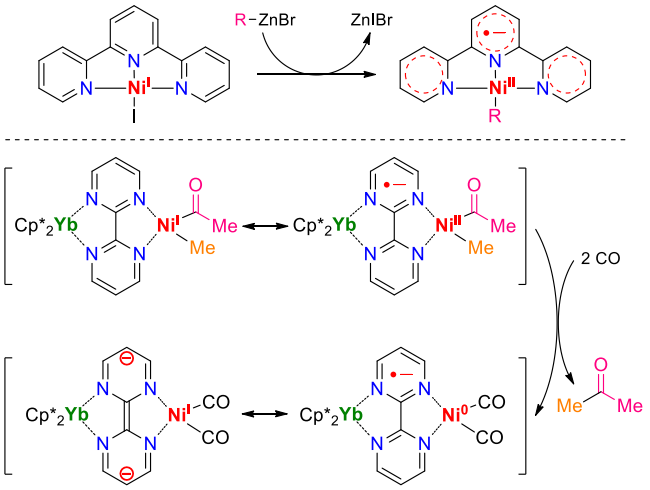

possesses one hole on the f-shell. The electronic structure of the heterobimetallic compound, $Cp^*_2Yb(bipym)NiMe_2$, was described as an open-shell singlet ground state—the two single electrons being antiferromagnetically coupled, while the triplet state being significantly populated at room temperature.[20]

Additionally, an important notion brought by this example is that spontaneous reductive elimination occurs, after migratory insertion of the CO in one methyl group, between the formed acyl and the remaining methyl fragment forming acetone and a low-valent Ni compound (Scheme 1, bottom). This situation is particularly appealing since further intramolecular single-electron transfer may occur, as illustrated in Scheme 1, adapting the oxidation state of the nickel-metal center.

In situ formation of metalloradical centers would be particularly interesting to test in alkene isomerization in light of the recent remarkable work of Schoenebeck, who used nickel chemistry for E-selective alkene isomerization.[22,23] The tour-de-force resided in the use of Ni(I) complexes judiciously stabilized by an NHC-type ligand, unraveling a new type of mechanism, a metalloradical-induced 1,3-H atom relocation, in which the nickel-hydride intermediate species has a limited lifetime, allowing chain-walking isomerization.[24] This system was recently employed to develop remote functionalization reactions,[22,25,26] while a related Ni(0)-phosphine catalytic system[27] was recently reported. The selectivity in alkene isomerization[28,29] remains indeed of great interest because of the versatility of the alkenes in the synthesis of materials for the pharmaceutical and food industry.[30] Usually, the transformation is achieved by the use of precious metals involving two electron pathways through metal-hydride or π-allyl (hydride shift) mechanisms.[31−33] Conversely, Holland showed that sterically encumbered cobalt complexes allow single-electron transfers that result in selective mono-isomerization, conversion of 1-alkene to 2-alkene, with Z-selectivity.[34,35]

In this article, we present the result of a ligand−metal electron shuttle, first allowing the *in situ* formation of low-valent nickel catalysts by reduction of the popular *N*-heteroaromatics-Ni(II) precatalysts with a borane, and second alkene isomerization with a significant selectivity toward mono-isomerization. The experimental and electronic mechanisms have been investigated and revealed an intermediate mechanism between the one proposed by Schoenebeck—a radical-induced 1,3-H relocation mechanism[23] and a π-allyl mechanism. The results described in this article analyze the role of the ligand electronics in the fine modulation of the catalyst reactivity and thus bring valuable information in the suitable choice of future ligands to be used.

Scheme 2. Reduction of 1 and 2 by HB(Cat)

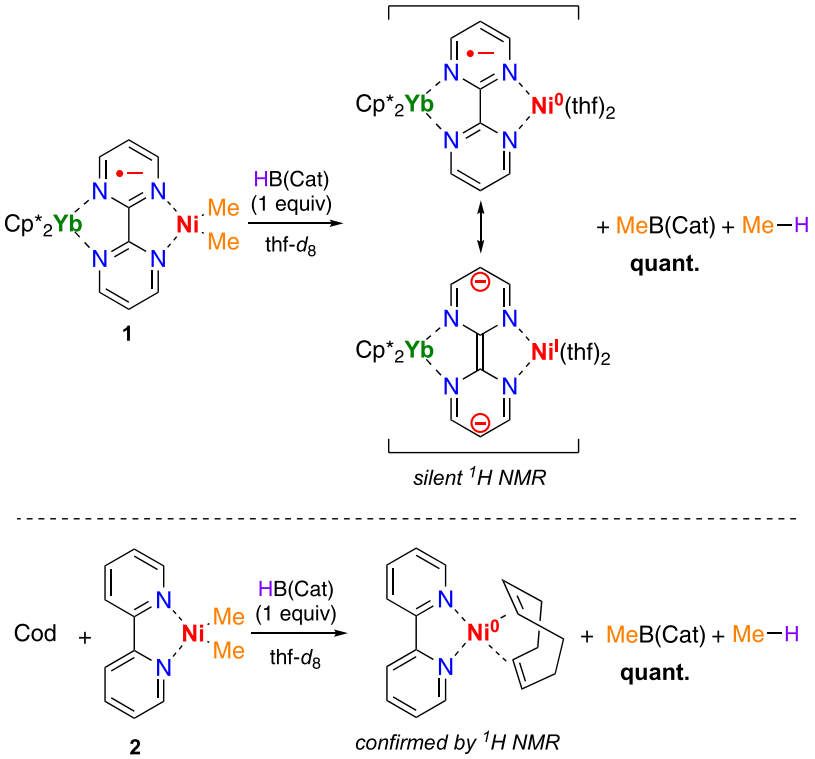

https://doi.org/10.1021/jacsau.2c00251
JACS Au 2022, 2, 1881−1888

2. RESULTS AND DISCUSSION

The production of Ni(0) catalysts from simple and stable Ni(II) precatalysts is a crucial step in nickel chemistry.[36] If possible, the substrates used shall be simple, cheap, and stable at ambient temperature as well as easy to handle. Examples in coupling reactions use reductants such as Zn, Mn, hydrides, or Grignard reagents.[37−39] The $Cp^*_2Yb(bipym)NiMe_2$, complex, **1**, is known to undergo oxidative additions followed by the fast elimination of ethane, while reductive elimination from acyl Ni(II) intermediates formed acetone and a supposed Ni(0) species at ambient temperature.[20]

Thus, the idea was to find a reagent that would easily form Ni(0) species from successive oxidative addition and reductive eliminations. Inspired by the hydroborylation and hydrosilylation chemistry,[1] both silane and borane were tested. While the silane does not react, HB(Cat) readily reacts with **1** to form a mixture of MeB(Cat) (Supporting information-Part III.a),[40] at 0.65 ppm, and methane, at 0.17 ppm, the products of two successive reductive eliminations after the oxidative addition of the borane on the $Ni(II)Me_2$ fragment. The reaction was monitored by ^{1}H NMR spectroscopy, and a titration confirmed that one equivalent only was necessary to suppress the signals of **1** and to form 1 equiv. of MeB(Cat) and methane (Scheme 2). Similar titrations were performed on the analogous $(bipy)NiMe_2$, **2**, complex, leading to a similar reactivity, although a black precipitate formed rapidly.

The formation of black powder probably resulted from the fast decomposition of Ni(0) in the absence of any stabilization group such as the divalent lanthanide Cp^*_2Yb fragment. Thus, when the reaction of **2** and HB(Cat) was performed in the presence of 1,5-cyclooctadiene (cod), a suitable diene ligand for the stabilization of Ni(0) species, the formation of the known (bipy)Ni(cod) was confirmed by ^{1}H NMR spectroscopy (SI-Part III.c).[41] The formal Ni(0) oxidation state of the species obtained after the reduction of **2** by the borane was confirmed by theoretical computations performed at the density functional theory (DFT) level of theory on the (bipy)Ni(Cod) complex (Figure S86). As expected for a $3d^{10}$ Ni(0) complex, the five highest occupied molecular orbitals (HOMOs) are mainly centered on the metal as it can be observed with the HOMO − 1, and HOMO, bonding orbitals between the Ni center and the Cod ligand, while the lowest unoccupied molecular orbital (LUMO) is mainly composed of the b_1 symmetry π^* orbital of the bipy ligand (in C_{2v} symmetry). Although the oxidation state of the Ni(0) center can be ascertained by NMR spectroscopy when **2** is reduced by the HB(Cat), no similar Cod trapping was observed when **1** was reduced by HB(Cat). In the latter case, the silent ^{1}H NMR spectrum prevents the assessment of whether the Cod ligand did coordinate the Ni center or not, and indicates that the proton relaxation is faster than with **1** itself, for which all proton signals were previously attributed. This would likely indicate the presence of another paramagnetic center in addition to the Yb(III) center. This agrees with the presence of a paramagnetic Ni(I) center rather than a diamagnetic Ni(0) center. To exclude the formation of a stable Ni−H species, two drops of CCl_4 were added after the reduction of **1** by HB(Cat), and no presence of chloroform was observed (Figure S12).

Considering that significant differences were observed between Ni(I) and Ni(0) alkene isomerization systems, the reactivity of both precatalysts (**1** and **2**) was tested on such reaction using allylbenzene (**A**) as the reference substrate (SI-Part IV).[42] The first observations showed high activity for **1** compared to **2**, which only led to poor conversion after several days (25%). Therefore, the optimization study was performed only with **1** (Scheme 3). Several different catalytic loadings were

Scheme 3. Optimal Catalytic Conditions and Preference for Mono-Isomerization

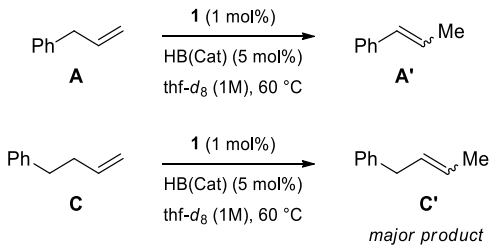

tested, and **1** proved to be efficient with a remarkably low catalytic loading down to 0.5 mol% (83% yield, 4.5 days). Thf-d_8 performed best as the reaction solvent, allowing the quantitative conversion and yielding the isomerized product in 16 h at 60 °C or in 3.5 days at 30 °C. Additionally, **1** was active for a long period (>1 week at 30 °C) while keeping a very high selectivity for the isomerization reaction. Only traces (<1%) of hydroboration side-products have been detected. Switching from **A** to 4-phenylbutene (**C**) led us to observe a selectivity toward the mono-isomerized product. No induction period was observed while monitoring the conversion rates by ^{1}H NMR. This means that once reduced, the Ni center readily performs the isomerization in the presence of the alkene (SI Part VI, Figure S52).

Intrigued by the absence of chain-walking isomerization and also by the nature of the nickel active species, mechanistic investigations were conducted to identify the mechanistic pathway that led to this peculiar reactivity. First, a conclusive mercury drop test demonstrated that the catalytic system was homogeneous. The addition of CCl_4 after the start of the reaction formed traces of chloroform, which would be indicative of a Ni−H intermediate (Figure 1A). However, a similar test with dihydroanthracene did not affect the kinetics of the reaction (Figures S14 and S56). The deuterium labeling experiment revealed no intermolecular hydrogen shift for **A-d_2** (SI-Part VII).[27] A scrambling experiment between **A-d_2** and **C** also indicated no deuterium incorporation in the isomerized product of **C** (Figure 1B), which is in good agreement with the metalloradical pathway described previously by Schoenebeck but could not exclude other mechanisms (Figure 1A).[23]

In light of the scrambling experiments, an important question remains in the role of the additional electron lying on the bipyrimidine ligand when it is coordinated to the reductive Cp^*_2Yb fragment in **1**.[20] In this case, the π^*-system of the bipym ligand, which is antibonding concerning the Ni d-orbital, is populated. In Pd chemistry, this is known to facilitate the oxidative addition, conferring a stronger donner character to the ligand,[19] while it can also facilitate radical-type reactivity.[12] Radical clock analyses performed on **1** with the ***cis*-I** substrate demonstrated that the reaction was indeed implying a radical with 34% of ***trans*-I** formed after 12 days (Figure 2).[23]

A control experiment was performed with the less reducing Cp^*_2Eu fragment instead of the Cp^*_2Yb one to form $Cp^*_2Eu(bipym)NiMe_2$, **3**, which was analyzed by X-ray diffraction. As identified by the silent ^{1}H NMR spectroscopy, typical of divalent europium, as well as the metrics of the bipym ligand (see the diagnostic $C-C_{bipym}$ distance, Table S3), **3** has

https://doi.org/10.1021/jacsau.2c00251
JACS Au 2022, 2, 1881−1888

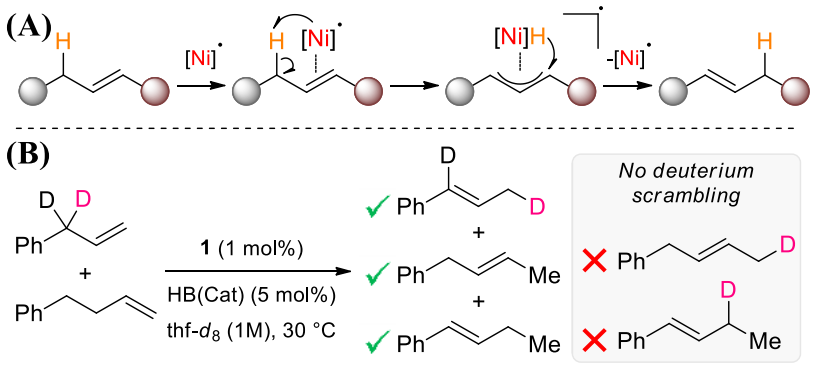

Figure 1. (A) Metalloradical-induced 1,3-H atom relocation. (B) Deuterium labeling cross-over experiment.

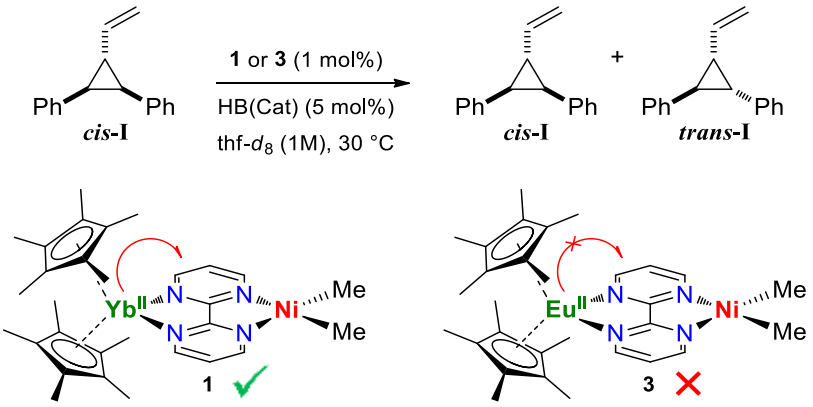

Figure 2. Radical clock experiments.

no electron on the bipym ligand. Similarly to **2**, **3** does not perform as well as **1** (Figure S51) in the isomerization reaction, implying that **1** has a unique electronic structure compared to **2** and **3**. The radical clock experiment with **3** only led to traces of ***trans*-I** (<2%) after several weeks (Figure 2). This ambiguous result does not strongly support a radical cyclopropyl opening, confirming a different electronic nature.

To summarize, it is known that the use of a Ni(I) catalyst allowed excellent chain-walking isomerization.[23] Both **2** and **3** have very limited reactivity in which no electron transfer is launched through the bipym ligand. However, **1** has a good but slow reactivity, which is significantly selective for the mono-isomerization. The electronic nature of **1** was thus in question. *In situ* EPR has been performed at a low temperature (10 K) on frozen tetrahydrofuran (THF) samples taken shortly after the addition of the HB(Cat) without (sample 1) and in the presence of the alkene substrate (sample 2). The results are shown in the SI. Very broad signals are typical of Yb(III), f^{13} sample, showing strong anisotropy. This is problematic since it can mask any signal that would be informative on the electronic structure of the catalytic resting state. Sample 1 has been simulated with a rhombic g tensor of 5.95, 2.41, and 1.64 with anisotropic hyperfine coupling. This corresponds well to a $Cp^*_2Yb(III)$ fragment coordinated to an *N*-heteroaromatic ligand,[43] but the radical, which is expected to be either on the bipym ligand or on the Ni center after electron transfer from the reductive Cp^*_2Yb fragment, is not observed at this temperature. Thus, the radical is likely coupled at a low temperature with the Yb(III) fragment. Sample 2 presents two species with two rhombic *g* tensors of 5.76, 2.77, and 1.78 and 4.40, 2.42, and 1.18, respectively. The presence of two ytterbium species under catalytic conditions is not surprising, but similarly, as in sample 1, the spectrum remains uninformative on the electronic structure because the ytterbium broad signals hide any possible signals from the nickel center. However, at higher temperatures (90 K), under catalytic conditions (after 5 days at 60 °C in the presence of the alkene and 1% **1**), the signals of the Yb(III), f^{13} typically decreased because of fast relaxation, leading to the appearance of the nickel signal (Figure S82). The rhombic signal (nearly axial) with g tensor features at $g = 2.22, 2.07$, and 2.03 ($g_{iso} = 2.11$) is typical of a metalloradical Ni(I) species with a significant orbital contribution.[23] This result shows that the Ni(I) species is the catalyst's resting state and that it is still active after 5 days at 60 °C, validating the quantitative results obtained after a long period (Table 1).

Theoretical computations were therefore performed at the DFT level (B3PW91), and the computed enthalpy profile at room temperature including the THF solvent is depicted in Figure 3. **1** was computed as both a triplet state and an open-shell singlet using the broken-symmetry approach since it is known that both are populated at room temperature.[20] The latter is found to be more stable than the triplet by 6.2 kcal/mol. This is further corroborated by CASSCF calculations distributing 14 electrons into 8 orbitals, which found the open-shell singlet lower in energy than the triplet by 4.5 kcal/mol. The removal of the two methyl fragments leads to an intermediate (**Int1**), which is lower in energy by 15.9 kcal/mol. The spin density is located on the ytterbium and the nickel centers, indicating the formation of a Ni(I) and a dianionic bipyrimidine ligand. This was likely to be driven by the spin pairing of the two electrons stored on the twice-reduced bipym fragment. **Int1** can bind THF solvent molecules, up to two, forming two stable

https://doi.org/10.1021/jacsau.2c00251
JACS Au 2022, 2, 1881−1888

Table 1. Conversion and yield of the major products[abcdef]

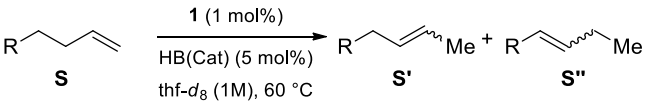

Starting material	Major product	Yield[b]	E:Z[b]	Conversion[b]
A	A'	96%[c] >99%[d]	99:1	4%[c] <1%[d]
B	B'	73%	-	12%
C	C'	64%[e] 48%	72:28[e] 79:21	4%[e] 1%
D	D'	50%	-	1%
E	E'	85%[e] 79%	65:35[e] 72:28	4%[e] 2%
F	F'	70%	-	16%
G	G'	41%	-	59%
H	H'	47%	N.D[f]	7%

[a]Reaction conditions: alkene (0.5 mmol), **1** (5 μmol), and HB(Cat) (25 μmol) in thf-d_8 (1M) at 60 °C during 5.5 days. [b]Determined by ^{1}H NMR using 1,3,5-tri-(*tert*-butyl)benzene or benzene as internal standards. [c]After 16 h. [d]After 3.5 days. [e]After 19 h. [f]Not determined.

intermediates (**Int2** and **Int3**). The coordination of the 4-phenylbutene *via* the removal of the THF molecules is again exergonic by 1.8 kcal/mol (**Int4**), which is the resting state of the catalytic reaction. The rate-determining step (**TS1**) with a barrier of 35.1 kcal/mol is the C−H activation step, which imposes a pseudo-π-allyl coordination of the alkene substrate, in which the unpaired spin density is distributed over the overall system Yb, bypim, and Ni, showing the importance of the redox fragment (electron shuttle) in its stabilization. The barrier is rather high, 11.0 kcal/mol above the one found for the Ni^I-NHC system,[23] in agreement with the slow reactivity at room temperature, which necessitates heating. Two intermediate species (**Int5** and **Int6**) have a similar structure to a Ni(II) hydride, a bipym radical ligand, and a π-allyl substrate. Between **Int5** and **Int6**, the difference is the necessary inversion of the hydride to relocate it close to the terminal methylene group. The second transition state (**TS2**) found corresponds to the hydrogen transfer to that latter methylene group. **TS2** recovers a similar electronic structure to **TS1** with a Ni(I)-dianionic bipym ligand, in which the spin density is firmly located on the Ni and Yb centers. Between **Int5** and **TS2**, the energy profile is flat within only 3 kcal/mol, which implies that the hydride rotation from **Int5** to **Int6** is barrierless, as observed with the system of Schoenebeck and co-workers. The mono-isomerized alkene adduct (**Int7**) is found downhill by 42.3 kcal/mol and only slightly exergonic compared to **Int4** (0.9 kcal/mol). The energy difference between the two alkene adducts explains well why the kinetics do not strictly follow first order but pseudo first order; when the concentration of the terminal alkene decreases, the exchange equilibrium between **Int4** and **Int7** is slower and the rate slows down. The second isomerization follows a similar path to a C−H activation transition state (**TS3**) of 33.2 kcal/mol, which is slightly lower than that of **TS1** (2.9 kcal/mol) but lies within the precision of the method (4−5 kcal/mol). From **TS3** to **TS4**, the hydrogen atom transfer step, the energy surface is also flat and the electronic structure is similar to what was described previously. The final product **Int10** is downhill by 25.1 kcal/mol, which means that **Int10** is 5.8 kcal/mol above **Int7**. This is due to the smaller donation from the styrene fragment to the Ni(I) in **Int10** compared to the donation of the internal olefin in **Int7**. This is well highlighted by the Ni−C Wiberg bond indexes (WBI), which are 0.1 and 0.4 in **Int10** and **Int7**, respectively.

The second isomerization is thus endothermic based on the olefin adduct that is formed (**Int10**). However, this does not prevent the kinetic formation of the styrene fragment (second isomerization step), which is accumulated because of the exchange equilibrium between **Int4**, **Int7**, and **Int10** *via* **Int2** or **Int3**. Indeed, in this particular case, the product of the second isomerization is more thermodynamically stable because of the formation of a stable fragment. As an additional note, the endothermicity of the second isomerization step (the first one is not) explains well the preference for the mono-isomerization when the product of the second isomerization step is not thermodynamics favored. The unusual electronic structure of a Ni(I) center coordinating alkenes is likely to play a role in this

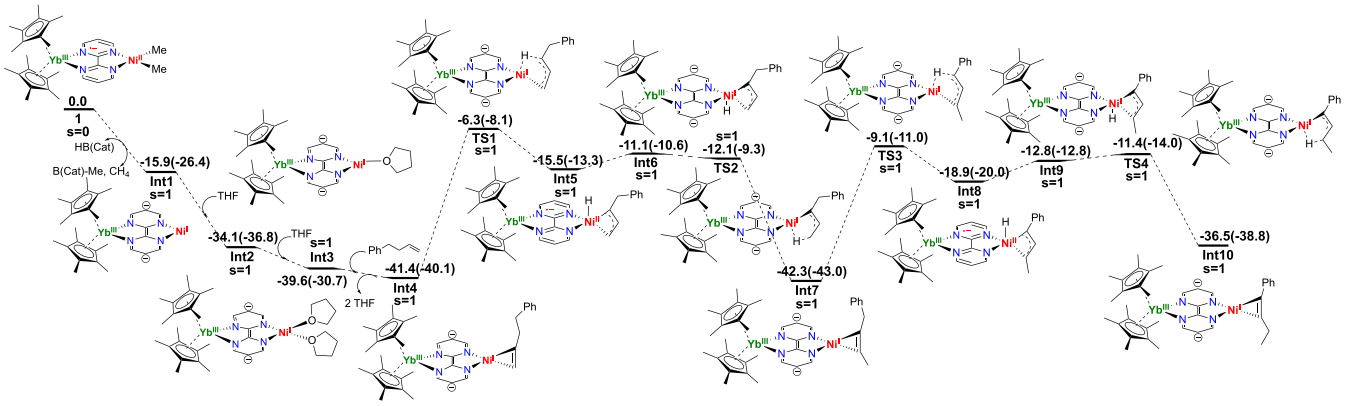

Figure 3. DFT-computed enthalpy profile (Gibbs free energy in parentheses) including the THF solvent and mechanism of the mono- and di-isomerization processes of the 4-phenylbutene induced by **1**.

https://doi.org/10.1021/jacsau.2c00251
JACS Au 2022, 2, 1881−1888

feature. This is rather interesting and provides a way to adapt the selectivity by adapting the ligand electronics to disfavor the internal alkene coordination. Prospective theoretical studies will be further used in this direction.

With this new mechanistic pathway in mind, various substrates were tested to assess the selectivity and efficiency (Table 1) of the transformation using the optimal conditions (1 mol % of **1**, 5 mol % of HB(Cat) in thf-d_8 at 60 °C, Scheme 2) described above (SI-Part V). Only unfunctionalized substrates were chosen to prevent the potential lack of compatibility between the organoytterbium moiety and oxygenated or halogenated functional groups. First, two substrates that can only perform mono-isomerization were chosen: allylbenzene (**A**) and 2-methylbut-1-ene (**B**). While **A** yielded nearly quantitively (96%) to **A′** in 16 h and complete conversion in 3.5 days at 60 °C, **B** was not entirely converted even after 5.5 days, indicating a strong influence of the steric hindrance. We then turned to substrates, for which several isomerization reactions are possible to access the mono-isomerization selectivity. The 4-phenylbutene (**C**) substrate was nearly completely converted (96%) in 19 h with a moderate selectivity of 2:1 ratio in favor of the mono-isomerized product **C′**, concurring with the theoretical studies highlighted above. The ratio dropped to 1:1 after 5.5 days of reaction because of the thermodynamic stability induced by the styrene fragment present in the **C″** product. On a similar line, the vinyl cyclohexane (**D**), showed a poor selectivity of 1:1 for the mono-isomerized product, while a quantitative conversion was reached after 5.5 days. This is also likely to be due to the thermodynamic stability of internal cyclic alkene fragments as all of the different isomerization products have been observed.

Thus, the selectivity for mono-isomerization was significantly improved when the thermodynamic driving force of the aromatic substitution was not present as in the hex-1-ene (**E**)/ a good selectivity of 8:1 in favor of **E′** was reached after 19 h of reaction with 96% conversion. Note that the selectivity only slightly decreased until 6:1 after 5.5 days of reaction, demonstrating well the endothermicity of the second isomerization reaction process. Similarly, a good ratio of 5:1 in favor of the mono-isomerized product was observed when a cyclic disubstituted alkene (**F**) was employed, although a slight decrease in yield can be noted, certainly due to the sterics of the substrate. In agreement with these observations, the use of a very hindered compound (**G**) led to a high selectivity (1:0) at the expense of a good yield (41%). Diene substrates were also tested, such as 4-vinylcyclohexene and 1,7-octadiene (Figures S44−S49). In the first case, the conversion was low, whereas, in the case of 1,7-octadiene, the interpretation of the NMR data did not allow us to conclude clearly about conversion and selectivity. In this matter, citronellene (**H**) is an excellent example to observe the different possible isomers formed also confirming the selectivity (1:1) of the catalytic system toward the mono-isomerization product (**H′**) in the case of diene substrates. Overall, the scope nicely concurs with the theoretical work, showing that the rate-determining step is the C−H activation, the energy cost of which is then impacted by the direct steric environment, while the selectivity is controlled by the energy of the final product versus that of the mono-isomerization one. This study shows that the electron shuttle on the ligand favors the control of the rate and selectivity of the reaction. Ligand's modification will then allow for improving the efficiency and/or selectivity of these catalysts.

3. CONCLUSIONS

In conclusion, the article reports the facile access to active low-valent Ni species from Ni(II)-*N*-heteroaromatics complexes as well as the efficient alkene isomerization with significant selectivity for the mono-isomerization with catalytic loading as low as 0.5%. In the heterometallic case, the reduced bipym ligand stabilizes the formally +I oxidation state for the Ni center, produced *in situ* by a simple borane reagent, as shown by radical clock experiments and theoretical computations. The outline of this article is the possibility for the *N*-heteroaromatic ligands to behave as a redox-active ligand, accommodating the spin density from the radical anionic form to the dianionic form, thus facilitating an electron shuttle from the ligand to the nickel center. The mechanism is found to be between the 1,3-H atom relocation, as recently demonstrated for Ni(I) species,[19] and a more classical π-allyl mechanism. The electron shuttle and formation of metalloradical Ni(I) species leads to a situation where the coordination of internal alkenes to the Ni center is less thermodynamically favorable than the coordination of terminal alkenes, thus proving a way to favor mono-isomerization. The new catalyst possesses a tunable redox-active ligand and a tunable low-valent lanthanide fragment; multiple combinations are thus possible to increase selectivity in alkenes isomerization. The report of a facile electron shuttle for Ni(I) species formation will allow several additional applications in catalysis, which shall be reported in due time.

■ ASSOCIATED CONTENT

Supporting Information

The Supporting Information is available free of charge at https://pubs.acs.org/doi/10.1021/jacsau.2c00251.

Syntheses, solution NMR data, kinetics, EPR data, computations, and structural information (PDF)
Structures (CIF)
Optimized_structures (XYZ)

■ AUTHOR INFORMATION

Corresponding Authors

Laurent Maron − *LPCNO, UMR 5215, Université de Toulouse-CNRS, INSA, UPS, 31077 Toulouse cedex 4, France*; orcid.org/0000-0003-2653-8557; Email: maron@irsamc.ups-tlse.fr

Grégory Danoun − *LCM, CNRS, Ecole polytechnique, Institut Polytechnique de Paris, Route de Saclay, 91120 Palaiseau, France*; orcid.org/0000-0003-2646-0091; Email: gregory.danoun@polytechnique.edu

Grégory Nocton − *LCM, CNRS, Ecole polytechnique, Institut Polytechnique de Paris, Route de Saclay, 91120 Palaiseau, France*; orcid.org/0000-0003-0599-1176; Email: gregory.nocton@polytechnique.edu

Authors

Maxime Tricoire − *LCM, CNRS, Ecole polytechnique, Institut Polytechnique de Paris, Route de Saclay, 91120 Palaiseau, France*

Ding Wang − *LCM, CNRS, Ecole polytechnique, Institut Polytechnique de Paris, Route de Saclay, 91120 Palaiseau, France*

Thayalan Rajeshkumar − *LPCNO, UMR 5215, Université de Toulouse-CNRS, INSA, UPS, 31077 Toulouse cedex 4, France*

Complete contact information is available at:

https://doi.org/10.1021/jacsau.2c00251
JACS Au 2022, 2, 1881−1888

https://pubs.acs.org/10.1021/jacsau.2c00251

Funding

This project has received funding from the H2020 European Research Council (ERC) under the European Union's Horizon H2020 research program (grant agreement no. 716314).

Notes

The authors declare no competing financial interest.

■ ACKNOWLEDGMENTS

Ecole Polytechnique and CNRS are thanked for funding. Dr. Christian Herrero is thanked for the help in the acquisition of the EPR data. L.M. is a senior member of the Institut Universitaire de France. CalMip is acknowledged for a generous grant of computing time.

■ REFERENCES

(1) Obligacion, J. V.; Chirik, P. J. Earth-Abundant Transition Metal Catalysts for Alkene Hydrosilylation and Hydroboration. *Nat. Rev. Chem.* **2018**, *2*, 15−34.

(2) Bour, J. R.; Ferguson, D. M.; McClain, E. J.; Kampf, J. W.; Sanford, M. S. Connecting Organometallic Ni(III) and Ni(IV): Reactions of Carbon-Centered Radicals with High-Valent Organonickel Complexes. *J. Am. Chem. Soc.* **2019**, *141*, 8914−8920.

(3) D'Accriscio, F.; Borja, P.; Saffon-Merceron, N.; Fustier-Boutignon, M.; Mézailles, N.; Nebra, N. C−H Bond Trifluoromethylation of Arenes Enabled by a Robust, High-Valent Nickel(IV) Complex. *Angew. Chem., Int. Ed.* **2017**, *56*, 12898−12902.

(4) Lipschutz, M. I.; Yang, X.; Chatterjee, R.; Tilley, T. D. A Structurally Rigid Bis(Amido) Ligand Framework in Low-Coordinate Ni(I), Ni(II), and Ni(III) Analogues Provides Access to a Ni(III) Methyl Complex via Oxidative Addition. *J. Am. Chem. Soc.* **2013**, *135*, 15298−15301.

(5) Mirica, L. M.; Smith, S. M.; Griego, L. Organometallic Chemistry of High-Valent Ni(III) and Ni(IV) Complexes. In *Nickel Catalysis in Organic Synthesis*; John Wiley & Sons, Ltd, 2020; pp 223−248.

(6) Camasso, N. M.; Sanford, M. S. Design, Synthesis, and Carbon-Heteroatom Coupling Reactions of Organometallic Nickel(IV) Complexes. *Science* **2015**, *347*, 1218−1220.

(7) Meucci, E. A.; Ariafard, A.; Canty, A. J.; Kampf, J. W.; Sanford, M. S. Aryl−Fluoride Bond-Forming Reductive Elimination from Nickel(IV) Centers. *J. Am. Chem. Soc.* **2019**, *141*, 13261−13267.

(8) Nebra, N. High-Valent NiIII and NiIV Species Relevant to C−C and C−Heteroatom Cross-Coupling Reactions: State of the Art. *Molecules* **2020**, *25*, No. 1141.

(9) Luca, O. R.; Crabtree, R. H. Redox-Active Ligands in Catalysis. *Chem. Soc. Rev.* **2013**, *42*, 1440−1459.

(10) Ray, K.; Petrenko, T.; Wieghardt, K.; Neese, F. Joint Spectroscopic and Theoretical Investigations of Transition Metal Complexes Involving Non-Innocent Ligands. *Dalton Trans.* **2007**, 1552−1566.

(11) Chirik, P. J.; Karl, Wieghardt Radical Ligands Confer Nobility on Base-Metal Catalysts. *Science* **2010**, *327*, 794−795.

(12) Broere, D. L. J.; de Bruin, B.; Reek, J. N. H.; Lutz, M.; Dechert, S.; van der Vlugt, J. I. Intramolecular Redox-Active Ligand-to-Substrate Single-Electron Transfer: Radical Reactivity with a Palladium(II) Complex. *J. Am. Chem. Soc.* **2014**, *136*, 11574−11577.

(13) van der Vlugt, J. I. Radical-Type Reactivity and Catalysis by Single-Electron Transfer to or from Redox-Active Ligands. *Chem. - Eur. J.* **2019**, *25*, 2651−2662.

(14) Jacquet, J.; Chaumont, P.; Gontard, G.; Orio, M.; Vezin, H.; Blanchard, S.; Desage-El Murr, M.; Fensterbank, L. C−N Bond Formation from a Masked High-Valent Copper Complex Stabilized by Redox Non-Innocent Ligands. *Angew. Chem., Int. Ed.* **2016**, *55*, 10712−10716.

(15) Jacquet, J.; Salanouve, E.; Orio, M.; Vezin, H.; Blanchard, S.; Derat, E.; Desage-El Murr, M.; Fensterbank, L. Iminosemiquinone Radical Ligands Enable Access to a Well-Defined Redox-Active CuII−CF3 Complex. *Chem. Commun.* **2014**, *50*, 10394−10397.

(16) Budnikova, Y. H.; Vicic, D. A.; Klein, A. Exploring Mechanisms in Ni Terpyridine Catalyzed C−C Cross-Coupling Reactions—A Review. *Inorganics* **2018**, *6*, No. 18.

(17) Jones, G. D.; Martin, J. L.; McFarland, C.; Allen, O. R.; Hall, R. E.; Haley, A. D.; Brandon, R. J.; Konovalova, T.; Desrochers, P. J.; Pulay, P.; Vicic, D. A. Ligand Redox Effects in the Synthesis, Electronic Structure, and Reactivity of an Alkyl−Alkyl Cross-Coupling Catalyst. *J. Am. Chem. Soc.* **2006**, *128*, 13175−13183.

(18) Lin, X.; Phillips, D. L. Density Functional Theory Studies of Negishi Alkyl−Alkyl Cross-Coupling Reactions Catalyzed by a Methylterpyridyl-Ni(I) Complex. *J. Org. Chem.* **2008**, *73*, 3680−3688.

(19) Goudy, V.; Jaoul, A.; Cordier, M.; Clavaguéra, C.; Nocton, G. Tuning the Stability of Pd(IV) Intermediates Using a Redox Non-Innocent Ligand Combined with an Organolanthanide Fragment. *J. Am. Chem. Soc.* **2017**, *139*, 10633−10636.

(20) Wang, D.; Moutet, J.; Tricoire, M.; Cordier, M.; Nocton, G. Reactive Heterobimetallic Complex Combining Divalent Ytterbium and Dimethyl Nickel Fragments. *Inorganics* **2019**, *7*, No. 58.

(21) Tilley, T. D.; Andersen, R. A.; Spencer, B.; Zalkin, A. Crystal Structure of Bis(Pentamethylcyclopentadienyl)Bis(Pyridine)-Ytterbium(II). *Inorg. Chem.* **1982**, *21*, 2647−2649.

(22) Guven, S.; Kundu, G.; Weßels, A.; Ward, J. S.; Rissanen, K.; Schoenebeck, F. Selective Synthesis of *Z* -Silyl Enol Ethers via Ni-Catalyzed Remote Functionalization of Ketones. *J. Am. Chem. Soc.* **2021**, *143*, 8375−8380.

(23) Kapat, A.; Sperger, T.; Guven, S.; Schoenebeck, F. E-Olefins through Intramolecular Radical Relocation. *Science* **2019**, *363*, 391−396.

(24) Larionov, E.; Lin, L.; Guénée, L.; Mazet, C. Scope and Mechanism in Palladium-Catalyzed Isomerizations of Highly Substituted Allylic, Homoallylic, and Alkenyl Alcohols. *J. Am. Chem. Soc.* **2014**, *136*, 16882−16894.

(25) Liu, C.-F.; Wang, H.; Martin, R. T.; Zhao, H.; Gutierrez, O.; Koh, M. J. Olefin Functionalization/Isomerization Enables Stereoselective Alkene Synthesis. *Nat. Catal.* **2021**, *4*, 674−683.

(26) Wang, H.; Liu, C.-F.; Martin, R. T.; Gutierrez, O.; Koh, M. J. Directing-Group-Free Catalytic Dicarbofunctionalization of Unactivated Alkenes. *Nat. Chem.* **2022**, *14*, 188−195.

(27) Iwamoto, H.; Tsuruta, T.; Ogoshi, S. Development and Mechanistic Studies of (E)-Selective Isomerization/Tandem Hydroarylation Reactions of Alkenes with a Nickel(0)/Phosphine Catalyst. *ACS Catal.* **2021**, *11*, 6741−6749.

(28) Otsuka, S.; Tani, K. Isomerization of Olefin and the Related Reactions. In *Transition Metals for Organic Synthesis*; John Wiley & Sons, Ltd, 1998; pp 147−157.

(29) Koley, D.; De, S.; Sivendran, N.; Gooßen, L. J. Isomerization of Functionalized Olefins by Using the Dinuclear Catalyst [PdI(μ-Br)(PtBu3)]2: A Mechanistic Study. *Chem. - Eur. J.* **2021**, *27*, 15227−15239.

(30) Vasseur, A.; Bruffaerts, J.; Marek, I. Remote Functionalization through Alkene Isomerization. *Nat. Chem.* **2016**, *8*, 209−219.

(31) Larionov, E.; Li, H.; Mazet, C. Well-Defined Transition Metal Hydrides in Catalytic Isomerizations. *Chem. Commun.* **2014**, *50*, 9816−9826.

(32) Biswas, S. Mechanistic Understanding of Transition-Metal-Catalyzed Olefin Isomerization: Metal-Hydride Insertion-Elimination vs. π-Allyl Pathways. *Comments Inorg. Chem.* **2015**, *35*, 300−330.

(33) Molloy, J. J.; Morack, T.; Gilmour, R. Positional and Geometrical Isomerisation of Alkenes: The Pinnacle of Atom Economy. *Angew. Chem., Int. Ed.* **2019**, *58*, 13654−13664.

(34) Chen, C.; Dugan, T. R.; Brennessel, W. W.; Weix, D. J.; Holland, P. L. Z-Selective Alkene Isomerization by High-Spin Cobalt(II) Complexes. *J. Am. Chem. Soc.* **2014**, *136*, 945−955.

(35) Kim, D.; Pillon, G.; DiPrimio, D. J.; Holland, P. L. Highly Z-Selective Double Bond Transposition in Simple Alkenes and

Allylarenes through a Spin-Accelerated Allyl Mechanism. *J. Am. Chem. Soc.* **2021**, *143*, 3070−3074.
(36) Montgomery, J. Nickel-Catalyzed Reductive Cyclizations and Couplings. *Angew. Chem., Int. Ed.* **2004**, *43*, 3890−3908.
(37) Weix, D. J. Methods and Mechanisms for Cross-Electrophile Coupling of Csp2 Halides with Alkyl Electrophiles. *Acc. Chem. Res.* **2015**, *48*, 1767−1775.
(38) Ritleng, V.; Henrion, M.; Chetcuti, M. J. Nickel N-Heterocyclic Carbene-Catalyzed C−Heteroatom Bond Formation, Reduction, and Oxidation: Reactions and Mechanistic Aspects. *ACS Catal.* **2016**, *6*, 890−906.
(39) Phapale, V. B.; Cárdenas, D. J. Nickel-Catalysed Negishi Cross-Coupling Reactions: Scope and Mechanisms. *Chem. Soc. Rev.* **2009**, *38*, 1598−1607.
(40) Ishida, K.; Yamazaki, H.; Hagiwara, C.; Abe, M.; Kusama, H. Efficient Generation and Synthetic Applications of Alkyl-Substituted Siloxycarbenes: Suppression of Norrish-Type Fragmentations of Alkanoylsilanes by Triplet Energy Transfer. *Chem. - Eur. J.* **2020**, *26*, 1249−1253.
(41) Binger, P.; Doyle, M. J.; McMeeking, J.; Krüger, C.; Tsay, Y.-H. Metallacycloalkanes: I. Preparation and Characterisation of α,A′-Bipyridyl-5-Nickela-3,3,7,7-Tetramethyl-Trans-Tricyclo[4.1.0.02,4]-Heptane. *J. Organomet. Chem.* **1977**, *135*, 405−414.
(42) Hassam, M.; Taher, A.; Arnott, G. E.; Green, I. R.; van Otterlo, W. A. L. Isomerization of Allylbenzenes. *Chem. Rev.* **2015**, *115*, 5462−5569.
(43) Nocton, G.; Lukens, W. W.; Booth, C. H.; Rozenel, S. S.; Medling, S. A.; Maron, L.; Andersen, R. A. Reversible Sigma C−C Bond Formation Between Phenanthroline Ligands Activated by (C5Me5)2Yb. *J. Am. Chem. Soc.* **2014**, *136*, 8626−8641.

https://doi.org/10.1021/jacsau.2c00251
JACS Au 2022, 2, 1881−1888